Biochimica et Biophysica Acta, 1102 (1992) 1–18

BBABIO 43644

Molecular analysis of dimethylsulfoxide reductase: a complex iron-sulfur molybdoenzyme of *Escherichia coli*

Joel H. Weiner, Richard A. Rothery, Damaraju Sambasivarao and Catharine A. Trieber

Department of Biochemistry, University of Alberta, Edmonton (Canada)

(Received 10 January 1992)

Key words: Molybdopterin; Iron-sulfur protein; Trimethylamine *N*-oxide; Electron transport; Anaerobic electron transport; Membrane protein

Contents

Correspondence to: J. Weiner, Department of Biochemistry, University of Alberta, Edmonton, Alberta, Canada, T6G 2H7.

Abbreviations: ANO, adenosine *N*-oxide; BV_{red}, reduced benzyl viologen; DHAP, dihydroxyacetone phosphate; $DMNH_2$, dimethylnaphthoquinol; DMSO, dimethylsulfoxide; DMS, dimethylsulfide; EPR, electron paramagnetic resonance spectroscopy; ETC, electron transfer chain; [Fe-S], iron-sulfur; G3P, glycerol 3-phosphate; HOQNO, 8-hydroxyquinoline *N*-oxide; MCD, magnetic circular dichroism spectroscopy; MetSO, methionine sulfoxide; MV_{red}, reduced methyl viologen; Moco, molybdopterin cofactor (complex of molybdenum with molybdopterin); MGD, molybdopterin guanine dinucleotide; MQ, menaquinone-8; TMAO, trimethylamine *N*-oxide; UQ, ubiquinone-8; $\Delta\mu_{H^+}$, proton electrochemical potential.

I. Introduction and Scope

The facultative anaerobe, *Escherichia coli*, is capable of inducing specialized respiratory chains when oxygen becomes limiting during growth. When grown anaerobically, with respiratory oxidants such as fumarate, nitrate or dimethylsulfoxide (DMSO), respiratory chains comprising a primary dehydrogenase (e.g., glycerol-3-phosphate dehydrogenase), an intermediate electron carrier, such as menaquinone or ubiquinone, and a specific terminal reductase, such as fumarate reductase, nitrate reductase or dimethylsulfoxide reductase, are synthesized [1–3]. The choice of the terminal electron acceptor is governed by the availability of these acceptors in the growth medium, as well as their redox potentials. In a given growth medium, the compound with the highest redox potential is preferred (Table I, [1]). The simplicity of the anaerobic respiratory chains, together with the ease of genetic manipulations in *E. coli*, have contributed significantly to the understanding of the mechanisms of energy transduction.

TABLE I

Midpoint potentials and free energy changes of alternative respiratory electron acceptors

$E_{m,7}$ and $\Delta G'_0$ values from [1].

Acceptor	$E_{m,7}$ (mV)	$\Delta G'_0$ (NADH as donor) (kJ mol^{-1})
Nitrate	+420	−146
DMSO	+160	−92
TMAO	+130	−89
Fumarate	+30	−67

The ability to reduce DMSO to dimethylsulfide (DMS), a major intermediate in the global sulfur cycle, is widespread in both prokaryotes and eukaryotes [4,5]. DMSO reductase (DmsABC) of *E. coli* is a complex membrane-bound, [Fe-S] molybdoenzyme [6–8], which catalyzes reduction of DMSO to DMS and also reduces a wide variety of *S*- and *N*-oxide compounds. Several other molybdoenzymes in *E. coli* also catalyze reduction of *S*- and/or *N*-oxides and confusion has surrounded the roles of these enzymes in energy transduction. Of these, DMSO reductase is well characterized at the biochemical, biophysical and molecular levels, and is proving to be an excellent model system for investigating the structure and mechanism of electron-transfer chain complexes. In this review we clarify the roles of *S*- and *N*-oxide reductases and summarize the current state of knowledge.

II. Ecology

Early studies on the global sulfur cycle suggested that half of the sulfur exists as reduced sulfide and that most of the reduced sulfide in the atmosphere is in the form of H_2S [9]. However, it is now believed that DMS is the major source of reduced sulfur and that it accounts for 50% of the total biogenic input of sulfur into the environment. It is emitted by oceans and plays a role in global climate control [10–12]. Much of the DMS is consumed by microorganisms in sea water and this helps to control the levels of DMS in the oceans [10]. DMSO arises naturally from photo-oxidation of DMS in the atmosphere or from phytoplankton degradation in marine environments [13]. DMSO is of low volatility and highly hygroscopic. It is therefore scavenged from the atmosphere by rain and returned to earth [12].

In addition to the natural sources of DMSO, a number of man-made processes contribute to its build-up in the environment. It is present as a waste product of paper mills, used as a solvent, used as a vehicle for the administration of drugs, and production of DMS occurs during the course of degradation of sulfur-containing pesticides. Delineation of the mechanism of DMSO reduction may contribute to our understanding of the overall global sulfur balance [5,9–12].

III. Bacterial DMSO reduction

DMSO reductase activity appears to be widespread in microorganisms. Most DMSO reductases have a broad substrate specificity, reduce both DMSO and trimethylamine *N*-oxide (TMAO) and contain molybdenum at their active centers [6,14–17]. Sambasivarao and Weiner (unpublished results) have screened the ECOR [18] collection of 72 different *E. coli* isolates by Southern blot hybridization using the *E. coli* DMSO reductase operon (*dms*ABC) as probe [19]. All strains examined were positive, indicating that DMSO reductase is ubiquitous in *E. coli*. This agrees with the earlier findings of Zinder and Brock [5] who examined the DMSO reductase activity in crude extracts of a number of *Enterobacteriaceae* using NADH as an electron donor. They found that all *E. coli* strains examined catalyze NADH-dependent DMSO reduction in crude extracts, although it is not certain if this activity is due to the DmsABC enzyme. Similarly, most strains of *Klebsiella* and *Pseudomonas* are able to reduce DMSO. However, only 1 of 40 *Salmonella* strains has the activity, although TMAO reductase is widespread in *Salmonella* [4]. Schultz and Weaver [20] examined the DMSO reducing activity of 96 strains of non-sulfur-reducing purple bacteria and found that the majority are able to reduce DMSO. Oren and Truper [14] have found that members of the halophilic archaebacteria, such as *Halobacter halobium*, are also capable of DMSO and TMAO reduction. Of these, DMSO and TMAO reductases from *E. coli*, *S. typhimurium*, *Rhodobacter (Rhodopseudomonas) capsulatus* and *R. sphaeroides* have been purified and characterized [4,8,16,17,21–24].

IV. Relation to other *S*- and *N*-oxide reductases

Comparison of the DMSO and TMAO reductases from diverse bacterial groups indicates several interesting features (Table II): (i) *E. coli* has three distinct reductase activities: DMSO, TMAO, and adenosine *N*-oxide (ANO) reductase; (ii) TMAO/DMSO reductase activity from other bacteria (with the exception of *Vibrio parahaemolyticus* [36]) resides in a single polypeptide chain that is periplasmically localized; (iii) all the reductases require molybdenum; (iv) [Fe-S] centers are absent in all TMAO/DMSO reductases examined thus far except the DMSO reductase of *E. coli*; and (v) participation of *b*- and/or a *c*-type cytochrome(s) is evident in the electron transport pathway for the soluble, periplasmically localized TMAO reductases from all sources.

Much confusion surrounds the interplay of DMSO, TMAO and ANO reductases in *E. coli*. This is due to the overlapping substrate specificities of these enzymes (Table II) and to the multiple forms of TMAO reductases reported in the literature [21,28]. *E. coli* has been reported to contain a constitutive TMAO reductase and three inducible forms of the enzyme [4]. TMAO reductase is very similar to DMSO reductase in catalytic activity and this overlap has added to confusion in the literature. Inducible TMAO reductase fails to utilize *S*-oxides and can sustain growth on TMAO or other *N*-oxides [31]. The enzymes differ in localization; TMAO reductase is a soluble enzyme in the periplasm, DMSO reductase is membrane-bound (Table II). TMAO reductase also lacks [Fe-S] clusters. DMSO will induce expression of TMAO reductase but not DMSO reductase [37,38]. DMSO reductase is a heterotrimer (native M_r 155000) expressed constitutively under anaerobic growth conditions [4,26].

DMSO reductase sustains growth on DMSO, methionine sulfoxide (MetSO) or other *S*- and *N*-oxides [31]. This enzyme accounts for the constitutive TMAO reductase activity and for growth on TMAO in a *torA* mutant [28]. Sambasivarao and Weiner [39] have proposed that 'DMSO reductase' replace the term 'constitutive TMAO reductase'. The major inducible TMAO reductase is a homodimer of 110 kDa subunits [22]. Although other polypeptide molecular weights have been reported [21], earlier values are probably in error, due to proteolysis. Recent studies with an antibody generated against the major inducible enzyme have shown that all three inducible forms are multimers of the same 110 kDa subunit and these multiple forms may arise from lysis, purification or growth differences [21,22,31].

Mutants defective in DMSO and/or TMAO reductase have been generated. Sambasivarao and Weiner [31,37] constructed a series of chromosomal deletions of *dms*ABC by combining in vitro deletion mutagenesis of the cloned operon with homologous recombination. This was carried out in both the wild type and in a *torA* mutant. Mutants deleted for any portion of the *dms* operon were unable to support anaerobic growth on DMSO but grew on TMAO. The *dms*/*torA* mutants were unable to support growth on DMSO and TMAO. These studies confirmed that the constitutive TMAO reductase is DMSO reductase. Recently, Daruwala and Meganathan [40] also constructed mutants in *E. coli* lacking DMSO reductase by transposon

TABLE II

Comparison of DMSO / TMAO reductases from various sources

Organism	Reductase	Characteristics	*S*- or *N*-oxide-supported anaerobic growth	Reference(s)
Escherichia coli	DMSO	Constitutive, membrane bound, cytoplasmically localized, heterotrimer Moco and [Fe-S] clusters, no evidence for cytochrome-mediated electron transfer [a], generates $\Delta\mu_{H^+}$ [b]	DMSO, TMAO, ANO, Methionine sulfoxide, pyridine *N*-oxide, 3-OH pyridine *N*-oxide, 4-picoline *N*-oxide	6,8,25–27
Escherichia coli	TMAO	Inducible, soluble, periplasmically localized, homodimer, Moco, *b*- and *c*-type cytochromes mediate electron transfer, ETC generates $\Delta\mu_{H^+}$	TMAO, ANO, Pyridine *N*-oxide, 3-OH pyridine *N*-oxide, 4-picoline *N*-oxide	21,22,28–30
Escherichia coli	ANO	Constitutive, localization (n.d.) [c], cytochromes (n.d.) Moco [d], ETC generates $\Delta\mu_{H^+}$	ANO	21,31
Salmonella typhimurium	TMAO	Inducible, soluble, periplasmically localized, homotetramer, cytochromes (n.d.), Moco, ETC generates $\Delta\mu_{H^+}$	TMAO	22
Proteus vulgaris	DMSO/ TMAO [e]	Inducible, soluble, periplasmically localized, Moco, subunits (n.d.), cytochromes (n.d.), ETC generates $\Delta\mu_{H^+}$	DMSO and TMAO	15,32
Alteromonas sp.	TMAO	Inducible, soluble, periplasmically localized, *c*-type cytochrome mediates electron transfer, subunits (n.d.), cofactor(s) (n.d.), ETC generates $\Delta\mu_{H^+}$	TMAO	33
Rhodobacter capsulatus	DMSO/ TMAO [e]	Constitutive, soluble, periplasmically localized, single subunit, Moco, *b*- and *c*-type cytochromes mediate electron transfer, ETC generates $\Delta\mu_{H^+}$	DMSO and TMAO	17,34,24
Rhodobacter sphaeroides	DMSO/ TMAO [e]	Constitutive, soluble, periplasmically localized, single subunit, Moco, *b*- and *c*-type cytochromes mediate electron transfer, ETC generates $\Delta\mu_{H^+}$	DMSO and TMAO	16,35

[a] *E. coli* DMSO reductase obtains reducing equivalents from menaquinol, whereas the periplasmically localized reductases obtain reducing equivalents from cytochrome constituents of their respective electron transport chains.

[b] *E. coli* DMSO reductase produces a $\Delta\mu_{H^+}$ from the scalar distribution of the sites of MQH_2 oxidation and DMSO reduction across the cytoplasmic membrane. The H^+ gradients produced by electron transfer chains terminating in the soluble, periplasmically localized enzymes indicated above, arise from cytochromes donating electrons either directly or indirectly to these terminal reductases.

[c] n.d., not determined.

[d] Based on the inhibitory role of tungstate during anaerobic growth on ANO (D.S. and J.H.W., unpublished observations).

[e] In these cases one enzyme is responsible for both DMSO and TMAO reduction.

insertion and showed that these mutants retain the inducible TMAO reductase activity.

Sagai and Ishimoto [21] and Yamamoto et al. [41] have described another *N*-oxide reductase which uses ANO. This enzyme appears to be distinct from the inducible TMAO reductase and DMSO reductase. A strain lacking both DMSO reductase and TMAO reductase is still able to grow on ANO and has ANO reductase activity, indicating that ANO reductase is a distinct activity [31]. It is expressed constitutively under anaerobic growth conditions, but the precise localization of this enzyme has yet to be determined. ANO reductase fails to utilize other *S*- and *N*-oxides as terminal electron acceptors during growth, even though

the purified enzyme was shown to reduce several *N*-oxides [21]. The reasons for this selective in vivo substrate specificity are not clear.

V. Bioenergetics of growth on DMSO

Early studies [4,5] suggested that DMSO could not be used as a terminal electron acceptor to sustain anaerobic growth in *E. coli*. Later investigations by Bilous and Weiner [6,25] showed that *E. coli* is able to grow on DMSO as sole terminal electron acceptor and that growth on DMSO leads to the formation of a proton electrochemical potential ($\Delta\mu_{H^+}$).

Table I summarizes the redox potentials and energy yields of growth on DMSO and a number of alternate terminal electron acceptors. It can be seen that DMSO, although poorer (in terms of $\Delta G_0'$) than nitrate, is better than fumarate or TMAO, which have been examined extensively as electron acceptors [1,4,42]. However, the order of $\Delta G_0'$ is not reflected in the doubling times of *E. coli* strain HB101, grown on glycerol-containing media. The doubling time is 7.5 h on glycerol-DMSO media but only 2.5 h on glycerol-fumarate media [6].

V-A. Electron donors

E. coli is capable of growing anaerobically on glycerol-DMSO medium [6]. The glycerol must be phosphorylated to glycerol 3-phosphate (G3P) prior to oxidation by the anaerobic G3P dehydrogenase encoded by the *glpACB* operon [1]. The glycerol can be replaced by H_2, formate and substrates which generate NADH, but apparently not by D- or L-lactate [6,25].

V-B. Quinones

Under anaerobic conditions the level of menaquinol (MQH_2) in the inner membrane increases and the level of ubiquinol (UQH_2) falls [1]. Most anaerobic terminal reductases, with the exception of nitrate reductase, accept reducing equivalents solely from MQH_2. Using *men* and *ubi* mutants, it was shown that anaerobic growth on TMAO requires MQH_2 and that UQH_2 cannot substitute [43,44]. Similar conclusions were reached on the role of MQH_2 in DMSO reduction (J.H.W., unpublished results).

V-C. Cytochromes

The role of cytochromes in *E. coli* anaerobic electron transport terminating in nitrate and TMAO reductases has been established. Nitrate reductase (NarGHJI) contains a cytochrome *b* subunit (NarI) which is required for electron-transfer from the quinone pool to the [Fe-S] centers of the enzyme [45]. Cells grown on TMAO or DMSO express elevated levels of a cytochrome *b*, as well as a novel cytochrome *c*-556, in the periplasm in wild-type strains. These cytochromes have been implicated in the transfer of reducing equivalents to the periplasmically localized TMAO reductase [34,38,46]. Growth of a double mutant, defective in DMSO and TMAO reductases on either substrate, led to induction of *b*- and *c*-type cytochromes (D.S. and J.H.W., unpublished results). However, the appearance of these cytochromes may be the result of indirect induction by these substrates, as there is no evidence for the participation of cytochromes in the DMSO reductase pathway. Other anaerobic electron transport pathways (e.g., ANO reductase) may require cytochromes for function in *E. coli* and this needs further attention.

The periplasmic DMSO reductase of *R. capsulatus* has been examined in some detail. This enzyme is a single subunit of 46 kDa, serves as an energy conserving terminal reductase and uses both DMSO and TMAO as substrates. The enzyme is distinct from the nitrate reductase of this organism [17], although both are molybdoenzymes. This enzyme appears to receive reducing equivalents from a *b*- and/or a *c*-type cytochrome in the periplasm. A cytochrome *c*-556 of 13 kDa with an $E_{m,7}$ of +105 mV, has been implicated in transferring electrons from the membrane-bound quinone pool to the periplasmic reductase [46]. A similar periplasmic monomeric (86 kDa), molybdenum-containing DMSO reductase from *R. sphaeroides* has been reported [16,35].

V-D. Model for the generation of the proton electrochemical potential

A model for proton electrochemical potential ($\Delta\mu_{H^+}$) generation by electron-transfer from G3P to DMSO is presented in Fig. 1. This mechanism relies on the scalar distribution of redox reactions across the cytoplasmic membrane to generate the observed $\Delta\mu_{H^+}$. The site of MQ reduction by G3P dehydrogenase is formally on the cytoplasmic side, whereas the site of MQH_2 oxidation is formally on the periplasmic side.

V-E. Stoichiometry

(i) Respiratory chain terminating in DMSO reductase (DMSO respiration)

Bilous and Weiner have measured the $H^+/2e^-$ ratio in whole cells using glycerol as the exogenous electron donor and DMSO as the terminal electron acceptor [25]. A $H^+/2e^-$ ratio of 2.9 was obtained. This could indicate the possibility of two proton translocation sites. This value compares with an $H^+/2e^-$ value of 3.3 for nitrate. Proton translocation is not inhibited by 5 mM cyanide or 0.37 mM azide, concentrations which inhibit the nitrate and oxygen

responses [1,42]. HOQNO, an inhibitor of quinone reduction, inhibits the response at 5.6 μM. As expected, this respiratory chain also generates proton gradients coupled to the reduction of its substrate analogs such as MetSO, TMAO, and ANO [25]. However, the $H^+/2e^-$ ratio determined for TMAO or ANO is in the range of 1.2–1.8, considerably lower than that obtained with DMSO (D.S. and J.H.W., unpublished results). Several factors could influence the measurements of $H^+/2e^-$ ratio. These include the relative impermeability of substrates [26,36], energy (H^+)-dependent uptake of substrates [47,48], the nature of the electron donor [49], age of the cell cultures, alkalinization due to product formation, strain variations and/or growth conditions [29].

(ii) Respiratory chain terminating in TMAO reductase (TMAO respiration)

Takagi et al. [29] have reported a stoichiometry of 2–3 H^+/TMAO using endogenous substrates as electron donors. Depletion of endogenous substrates causes a rapid decrease in $H^+/2e^-$ ratio. As it is now evident that wild-type *E. coli* strains also express DMSO reductase [25,31], the overlapping substrate specificity of these reductases hinders direct interpretation of these data. Bilous and Weiner [25] distinguished DMSO- and TMAO-dependent respiration in wild-type cells, based on the susceptibility of these respiratory chains to the inhibitor HOQNO. While DMSO reductase is totally inhibited, respiratory chains terminating in nitrate and TMAO reductases are insensitive to HOQNO. Similar conclusions were reached in studies using a strain with a chromosomal deletion of the *dms* genes (D.S. and J.H.W., unpublished results).

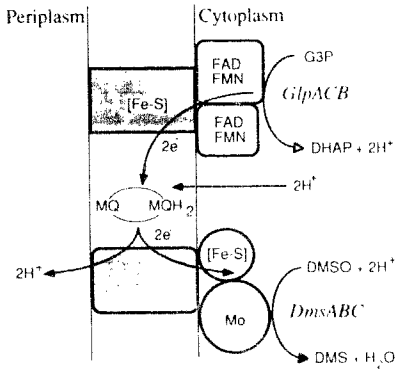

Fig. 1. Model for the vectorial generation of a proton electrochemical potential during anaerobic respiration. The periplasmic and cytoplasmic aspects of the *E. coli* inner membrane are shown with the primary dehydrogenase (G3P dehydrogenase, open squares) and a terminal reductase (DMSO reductase, open circles). These trimeric enzymes comprise two membrane extrinsic subunits and an integral membrane polypeptide (shaded area). The associated cofactors are shown within the depicted subunits. Subunits are not drawn to scale. The lipid-soluble carrier, MQ, is shown to mediate electron transfer from G3P dehydrogenase to DMSO reductase as well as to transfer protons generated by the dehydrogenase from the cytoplasm to the periplasmic compartment.

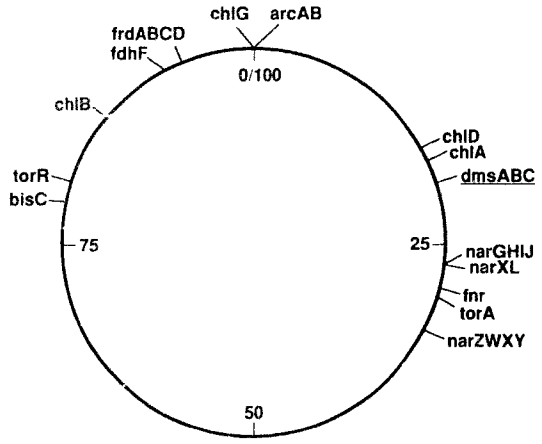

Fig. 2. The chromosome of *E. coli* with the relevant genes marked. *bisC*, biotin sulfoxide reductase; *chlA, B, D* and *G* steps in molybdopterin cofactor biosynthesis; *dmsABC*, DMSO reductase; *fdhF*, formate dehydrogenase; *fnr*, positive gene activator; *frdABCD*, fumarate reductase; *narGHIJ*, nitrate reductase; *narXL*, regulator of nitrate repression of DMSO reductase; *torA*, TMAO reductase.

VI. Molecular genetics of the dms operon

VI-A. Mapping of the dms operon

The structural genes for DMSO reductase (*dmsABC*) have been subcloned from the Clarke and Carbon plasmid colony bank into a variety of plasmid vectors as a 6.5 kb insert [7,19]. This clone over-expresses both DMSO and TMAO reductase activities about 15-fold and expresses the three Dms polypeptides, DmsABC, in in vitro transcription/translation studies. The restriction endonuclease map of this region has been compared to a total restriction map of *E. coli* and the *dms* operon has been unambiguously placed on a 210 kb *Not*I fragment. This locates *dmsABC* at 20′ near *rpsA* and *ompF* (Fig. 2). This map location differs from the location of *torA*, which is at 28′.

VI-B. Other genes required for DMSO reductase

Several genes have been identified which are essential for growth on DMSO and/or DMSO reductase activity. *chlA, B, E,* and *G* (Fig. 2), which are involved in molybdopterin biosynthesis, are all required and this was the first indication that DMSO reductase contains a molybdenum cofactor (Moco) [6]. Expression also requires the *fnr* gene, a positive regulator of several anaerobic activities [50–52] and is repressed by nitrate

via the *narX/narL* genes [53–55]. The enzyme is expressed in a *torA* mutant and is not affected by mutations in *narGHJI*. Growth on DMSO is also prevented by mutations in MQ biosynthesis but not by mutations in UQ, heme or siroheme biosynthesis.

VI-C. Organization of the operon

The DNA sequence of the 6.5 kb fragment encoding DMSO reductase has been determined by Bilous et al. [19]. A structural operon consisting of three open reading frames, encodes polypeptides with M_r values of 87350, 23070 and 30789 (Fig. 3). Preceding the predicted ATG start of *dmsA* is a GGCGG Shine-Delgarno sequence. The ribosome binding site of *dmsB* overlaps the *dmsA* stop codon and similarly the signal for *dmsC* overlaps *dmsB*. A transcriptional start site has been determined by Eiglmeier et al. [50], 218 nucleotides upstream from the initiating ATG. This is an unusually long 5′ untranslated region and the reason for this is unclear. The transcriptional start is preceded by a typical −10 region, but a consensus −35 region is not present. This is typical of genes that are under positive regulation [52]. Eiglmeier et al. predicted an Fnr binding site (Fnr box) about 40 base pairs upstream of the transcriptional start and a narL binding site very near the −10 region (Fig. 3). Seven base pairs following *dmsC* is a classical ρ-independent transcriptional terminator, comprising a symmetrical G-C rich region preceding a stretch of T residues [19].

Examination of the organization of the polypeptides encoded by the *dms* operon indicates that the architecture of the operon closely parallels that seen for the operons encoding fumarate reductase [2,7,56], both nitrate reductases [45,57], and formate dehydrogenase N [58] of *E. coli*. In all cases, the 5′ proximal gene (*dmsA, frdA, narG, narZ, fdnG*) encodes a large catalytic subunit which contains an electron-collecting cofactor, Moco or FAD, able to undergo a one- or two-electron oxidation-reduction (Section X). The next gene (*dmsB, frdB, narH, narY, fdnH*) encodes an electron-transfer subunit and this subunit has groups of Cys residues which ligate [Fe-S] clusters (see Section XI). The distal gene(s) (*dmsC, frdCD, narI, narV, fdnI*) encode the membrane anchor portion. These subunits zig-zag across the membrane several times and not only anchor the soluble catalytic subunits to the membrane but also bind quinone and stabilize the catalytic subunits (see Section XII). The architecture is not completely homologous. In fumarate reductase the anchor function is contained in two closely associated subunits. Nitrate reductase and formate dehydrogenase contain a cytochrome *b* (*NarI, FdnI*) which is not found in the other enzymes, and *nar* encodes a fourth subunit (*narJ*) which is necessary for the formation of the active enzyme [59,60].

VII. Regulatory mechanisms

It has been known for some time that *E. coli* selects the most efficient energy generating system for a par-

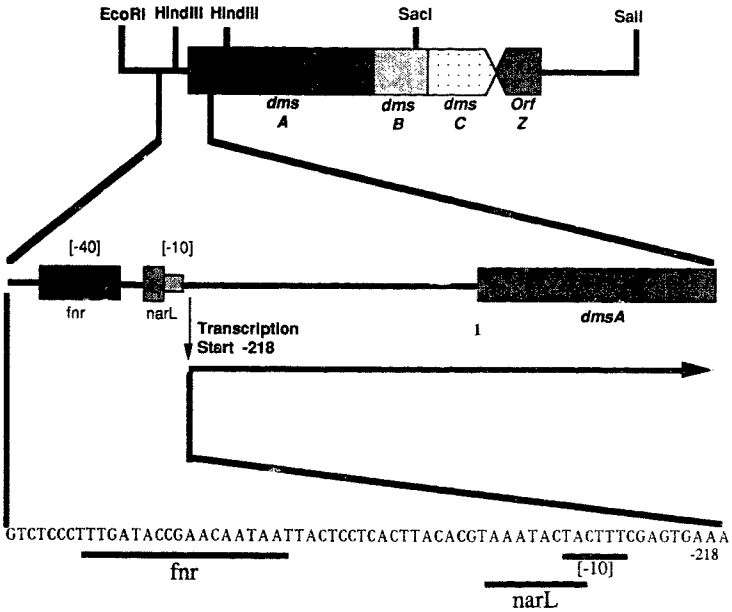

Fig. 3. Organization of the *dms* operon. The *Eco*RI and *Sal*I fragment of the recombinant plasmid pDMS222 carrying the structural genes *dmsABC* is depicted [19,50]. The organization of the promoter region and the sequences required for Fnr and NarL binding are shown.

ticular environment [54]. Fermentation is the most wasteful form of energy metabolism, as energy is only derived from substrate-level phosphorylation reactions. When an exogenous electron acceptor such as O_2, nitrate, DMSO or fumarate is available the cell will switch to respiration in which the reducing equivalents in NADH or exogenous electron donors are conserved by coupling the electron-transfer reactions to the formation of the $\Delta\mu_{H^+}$ [1]. *E. coli* will use the most positive acceptor available. Thus O_2/H_2O ($E_{m,7}$ = +0.82 V) will be used in preference to nitrate/nitrite ($E_{m,7}$ = +0.420 V), DMSO/DMS ($E_{m,7}$ = +0.16 V) or fumarate/succinate ($E_{m,7}$ = +0.031 V), and nitrate will be used in preference to fumarate or DMSO. There does not seem to be any selection between DMSO, TMAO and fumarate, although TMAO reductase is induced by TMAO in the medium [25,41]. DMSO reductase is expressed constitutively under anaerobic conditions [6–8].

VII-A. Fnr

DMSO reductase is induced about 65-fold by anaerobiosis via a positive gene activator protein (Fnr) and Eiglmeier et al. have shown that this is due to an increase in *dms* mRNA transcription [50]. This protein is a global regulator, which induces the expression of several anaerobic enzymes, including nitrate reductase, fumarate reductase, cytochrome *bd* [52,61], but not TMAO reductase [62]. It also represses the expression of selected aerobic enzymes, such as cytochrome *bo* [63,64]. Fnr is a constitutively expressed protein of 30 kDa and is composed of two domains. A carboxy proximal domain very similar to the cAMP catabolite gene activator protein (CRP) protein, which mediates cAMP-dependent catabolite repression. This portion has the helix-turn-helix motif characteristic of DNA binding proteins [65–67]. The amino proximal domain is specific to Fnr and contains a group of Cys residues which may coordinate an Fe^{2+} ion. It has been suggested that the anaerobic switch is mediated via an Fe^{3+}-Fe^{2+} interconversion [61,65,68–71]. By examination of a number of Fnr-dependent proteins Eiglmeier et al. [50] have identified an inverted repeat consensus sequence, TTGAT-ATCAA, which is the most likely Fnr binding site (Fig. 3). The presence of an inverted repeat indicates that Fnr probably binds as a dimer [72].

VII-B. NarL / NarX

As mentioned above, *E. coli* selects the most efficient energy generating system for a particular environment. Thus nitrate, with a higher redox potential, will repress DMSO reductase. This level of regulation is mediated by a two-component regulatory system encoded by the *narX* and *narL* genes [54,55]. Iuchi and Lin [54] originally reported that, under anaerobic conditions, *narL* induced nitrate reductase and repressed fumarate and TMAO reductases. These observations were extended to the *dms* operon by Cotter and Gunsalus [73], using *dms-lacZ* fusions. *narX* and *narL* are two adjacent genes mapping at 27′ on the *E. coli* chromosome. They encode polypeptides of 66 and 23 kDa, respectively [74]. *narX / narL* are similar to members of two-component regulatory families such as *ompR / envZ* [75] or *cheA / cheY* [76]. NarX is the 'sensor' and detects the availability or change in the environmental signals; nitrate and molybdate [74,77]. NarL is the 'receiver', and on a phosphorylation signal from NarX, activates or represses the transcription of sensitive genes by binding to a specific DNA sequence. Recently, Egan and Stewart [55] have examined the *narL / narX* operon in more detail. They found that the operon has a complex promoter structure and that *narX* may not be essential for nitrate regulation. Kalman and Gunsalus [74] have isolated mutants termed *narX**, which repress the *dms* operon, even in the absence of nitrate. They have also isolated mutations in *narX* which no longer respond to molybdate. Taken together, the results of Egan and Stewart [55] and Kalman and Gunsalus [74] suggest that two redundant sensors exist, both of which transduce a signal to *narL*. Egan and Stewart have proposed the existence of an additional sensor gene, *narQ* [55].

The NarL binding sequence or box has not been identified for the *dms* operon but current evidence suggests that the sequence is 5′ to the transcription initiation site at nucleotide −218 (Fig. 3) and just downstream of the Fnr box. It partially overlaps the −10 portion of the Shine-Delgarno RNA polymerase binding site [78].

VII-C. TorR

Yamamoto et al. [79] have described a gene, which they call *torR*, mapping close to *fdhA* at 80′ on the *E. coli* chromosome (Fig 2). This gene appears to be necessary for *dmsABC* expression, as well as for expression of the inducible TMAO reductase, nitrate reductase and the two formate dehydrogenases. The authors have suggested that the *torR* gene product provides an additional level of positive regulation of *dmsABC*. Although the level of molybdenum cofactor is normal in a *torR* mutant, it is unclear if this mutation resides in an enzyme, which catalyzes a modification of the cofactor, or its specific insertion into the polypeptides of the affected enzymes. Pascal et al. [80] have described a regulatory gene mapping at 22′ which they also call *torR*. This gene affects only the expression of the inducible TMAO reductase and must be distinguished from the gene described by Yamamoto et al. [79].

VII-D. ArcAB

ArcA and ArcB are members of a two-component regulatory system which represses aerobic genes under anaerobic conditions [52,54]. There is no evidence that this global regulator modulates DMSO reductase expression.

VIII. Enzymology of DMSO reductase

DMSO reductase was originally purified from the crude envelope fraction of cells over-expressing the activity by a combination of chromato-focusing and DEAE cellulose chromatography [8]. The enzyme is a heterotrimer of the DmsABC subunits and catalyzes DMSO-dependent oxidation of reduced benzyl viologen (BV_{red}). It has a very broad substrate specificity and is able to reduce many *S*- or *N*-oxide compounds, as well as chlorate. Maximal activity is observed with TMAO but the enzyme has the lowest K_m for DMSO: 180 μM vs. 700 μM [8]. Subsequent examination of this preparation by electron paramagnetic resonance spectroscopy (EPR) indicated that at least one of the [Fe-S] clusters is destroyed during the purification by the acidic pH used in the chromato-focusing step [27]. In addition, this enzyme was unable to catalyze DMSO-dependent oxidation of $DMNH_2$, a quinone analogue. A new purification was devised [27], using a combination of DEAE cellulose and gel exclusion chromatography. This preparation, which is about 90% homogeneous, is also a heterotrimer of DmsABC, has an identical EPR spectrum to the membrane-bound reductase, and catalyzes the oxidation of $DMNH_2$ [27].

BV_{red}, methyl viologen (MV_{red}) and $DMNH_2$ are efficient electron donors and exhibit a stoichiometry of $2BV_{red}$/DMSO, $2MV_{red}$/DMSO and 1 $DMNH_2$/DMSO. Activity is stimulated 3-fold by 300 μM ferrous iron. Exogenous ammonium molybdate has no effect. Optimal activity is obtained at pH 6.8 with Mops (3-[*N*-morpholino]propanesulfonic acid) buffer, whereas potassium phosphate buffer inhibits activity [6,8,27] and this accounts for the lower specific activity of earlier enzyme preparations.

Some comparison can be made with the enzymatic properties of DMSO/TMAO reductases from other organisms. While the *E. coli* DMSO reductase does not accept electrons from $FADH_2$, $FMNH_2$, or NADH, the enzyme from *Vibrio parahaemolyticus* can use these donors [21,23,34,36]. The activity of DMSO reductase from marine organisms can be detected after polyacrylamide gel electrophoresis under denaturing conditions [17]; however, the *E. coli* enzyme is very susceptible to SDS denaturation and all activity is lost at 0.001% SDS. The TMAO reductase activities of *S. typhimurium* and *E. coli* withstand incubation at 65°C, but DMSO reductase loses 90% of its activity when incubated at 65°C for 5 min.

IX. Topological organization of DMSO reductase

Everted vesicles isolated from bacteria over-expressing DMSO reductase are studded by dumb-bell type structures randomly arranged over the membrane, as judged by negative stain electron microscopy (Fig. 4). The structures are not seen in the wild-type [81] or in strains deleted for the DmsC polypeptide, and were shown to be the DmsAB subunits by immunogold electron microscopy with anti-DmsA or anti-DmsB antibodies [26]. These studies suggest that DmsA and B form a side-by-side dimer on the cytoplasmic surface, which is held to the membrane by the integral DmsC subunit (Fig. 5). The cytoplasmic surface location has been confirmed by a combination of thin-section immunogold electron microscopy, antibody labelling, proteolytic digestion, substrate accessibility, and lactoperoxidase catalyzed iodination [26]. Recently, EPR studies using the paramagnetic broadening reagent, dysprosium(III), have confirmed the cytoplasmic location of the molybdenum center and [Fe-S] clusters (W.J. Ingledew and J.H.W., unpublished results).

X. DmsA

dmsA is the promoter proximal gene in the *dms* operon and encodes a polypeptide with M_r 87350. DmsA is most likely the catalytic subunit based on architectural similarity to other terminal reductases [19].

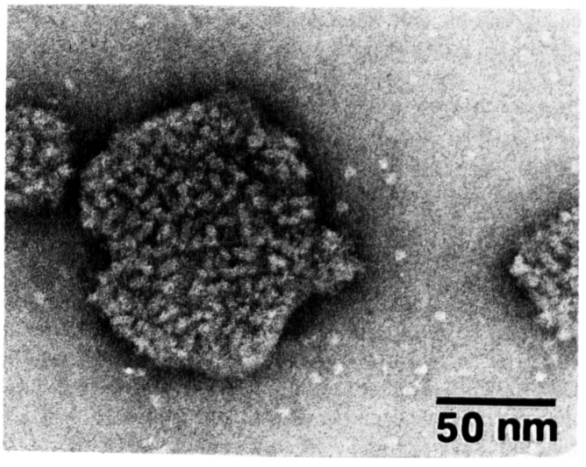

Fig. 4. Negative stain electron micrograph of everted inner membrane vesicles showing dumb-bell shaped extrinsic subunits (DmsAB) of DMSO reductase. Anaerobic growth of *E. coli* strain HB101 harboring the entire *dms* operon on a recombinant plasmid resulted in the amplification of the reductase subunits. Purified membrane vesicles prepared by French pressure lysis followed by sucrose density gradient centrifugation were negatively stained using 2% phosphotungstate [26].

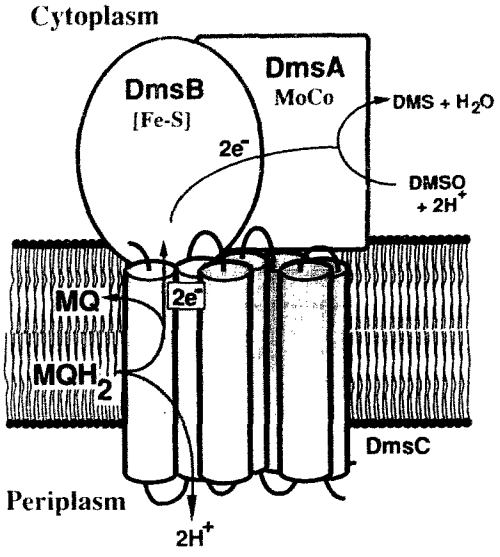

Fig. 5. Topological model for DMSO reductase in the inner membrane of *E. coli*. The catalytic subunits, DmsAB, are located on the cytoplasmic face of the inner membrane and contain Moco and [Fe-S] centers, respectively. The integral membrane subunit, DmsC, has seven or eight transmembranal helices (seven helices are shown here as cylinders) and mediates electron transfer from MQH_2 to the catalytic dimer.

X-A. The molybdenum cofactor

All living organisms require molybdenum as a key component of a variety of enzymes [82]. Several lines of evidence indicate that DmsA contains Mo. Initial studies by Bilous and Weiner [6] showed that *E. coli* is unable to grow anaerobically on DMSO in the presence of 10 mM tungstate. Cells grown on fumarate in the presence of tungstate are unable to express active DMSO reductase, TMAO reductase, or nitrate reductase, whereas fumarate reductase expression is normal. The need for Mo was confirmed by examination of the *chlA, B, E* and *G* mutations [80]. Mutations at these four loci block either cellular uptake and insertion of Mo into enzymes (*chlG*) or the biosynthesis of the molybdopterin (*chlA, chlB* and *chlE*) [83]. The *chlA, chlB* and *chlE* mutants are unable to grow on DMSO while the *chlG* mutant grows slowly after a 40 h lag [6]. The molybdenum cofactor of DMSO reductase has been further characterised both optically and by EPR (Section XB). Optical and fluoresence spectra (Fig. 6) indicate that the structure of the cofactor released from the enzyme after treatment with I_2 and KI is similar to that of the molybdenum cofactor released from sulfite oxidase [8,85]. The released cofactor has absorption maxima at 283 and 357 nm, and a fluoresence emission maximum at 443 nm when excited at its excitation maximum of 357 nm.

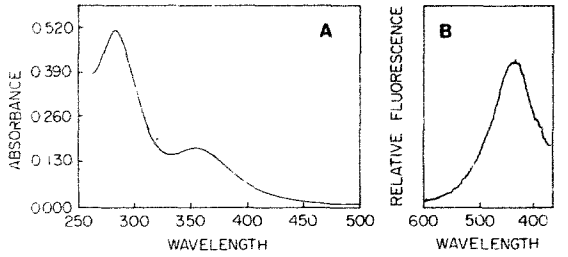

Fig. 6. Ultraviolet absorption and fluorescence emission spectra of the molybdenum cofactor extracted from *E. coli* DMSO reductase. The cofactor was released from the enzyme by boiling in the presence of KI and I_2 [84]. (A) Ultraviolet absorption spectra of extracts in 50 mM sodium phosphate buffer, pH 6.8. (B) Fluorescence spectrum of the extracted cofactor. The excitation wavelength was 357 nm, and the relative fluorescence was measured between 380 and 600 nm in 50 mM sodium phosphate buffer (pH 6.8). Reproduced from Ref. 8, with permission.

In all enzymes except the nitrogenases, Mo forms a complex with organic pterin, molybdopterin to produce the active molybdopterin cofactor, Moco. Moco is extremely unstable in the presence of oxygen and this has limited studies with the purified, intact cofactor [86]. The probable structure of Moco has been determined from the characterization of stable, inactive derivatives (Fig. 7a) [86]. The structure is composed of a pteridine derivative with a terminal phosphate group. Mo is bound via two thiolate ligands. Two oxo groups (or one oxo and one sulphido) are ligated to the Mo, leaving two coordination sites available for protein ligation [82]. Recent studies on the Moco of several bacterial enzymes indicate that it may differ from the eukaryotic

(a) Molybdopterin - MoCo

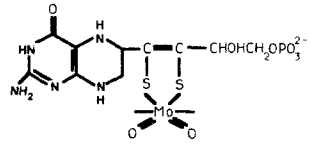

(b) Molybdenum Guanine Dinucleotide - MGD

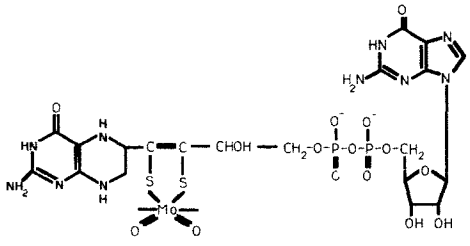

Fig. 7. Proposed structure of the molybdopterin cofactor, Moco [86], (a) and the molybdopterin guanine dinucleotide cofactor, MGD [87–91]. (b).

cofactor by the addition of guanosine, cytosine, adenosine or hypoxanthine monophosphate in a pyrophosphate linkage to the terminal phosphate of Moco (Fig. 7b) [87–91]. Recent observations of Johnson et al. [90] indicate that the *chlB* gene is required for synthesis of the molybdopterin guanine dinucleotide (MGD). Further, the DMSO reductase of *Rhodobacter sphaeroides* has been shown to contain MGD [87]. It is most likely that the *E. coli* DMSO reductase also contains a molybdopterin dinucleotide form of the cofactor based on the necessity of *chlB* for anaerobic growth on DMSO.

The *nit-1* mutation of *Neurospora crassa* synthesizes an inactive apo-nitrate reductase lacking Moco. Moco derived from a wide variety of sources is able to reconstitute nitrate reductase activity, providing a bioassay for Moco [92]. The cofactor released by denaturation of DMSO reductase can reconstitute nitrate reductase activity [8].

The reduction of DMSO to DMS requires the simultaneous availability of two electrons and these are provided by Mo(IV) in DmsA. Molybdenum can exist as the oxidized Mo(VI), the partially reduced Mo(V) (which is EPR detectable, subsection X-B) and the fully reduced Mo(IV). The intermediate state allows Mo to receive individual electrons from the one electron donor [Fe-S] centers in DmsB and this function is analogous to the semiquinone states of FAD in other reductases, such as fumarate reductase [2].

X-B. EPR characterization of the molybdenum cofactor

EPR studies of DMSO reductase provide additional support for DmsA being the site of Moco binding [27]. Preparations enriched in DmsA have strong molybdenum signals but severely reduced [Fe-S] signals, indicating that DmsA contains the Mo and that the [Fe-S] clusters are located elsewhere in the protein.

Mo (V) has a characteristic EPR spectrum (Fig. 8); thus, EPR is of great use in studies of molybdoenzymes. This information, coupled with EXAFS (extended X-ray absorption fine structure spectroscopy), comprises most of what is known about the environment of Mo in these enzymes [82]. The *g*-values and midpoint potentials determined for *E. coli* DMSO reductase are compared with two other prokaryotic molybdoenzymes, *E. coli* nitrate reductase and *R. sphaeroides* DMSO reductase in Table III. Both of the *E. coli* enzymes have other prosthetic groups ([Fe-S] clusters and a heme in nitrate reductase) which interfere with most spectroscopic studies of the molybdenum center [82].

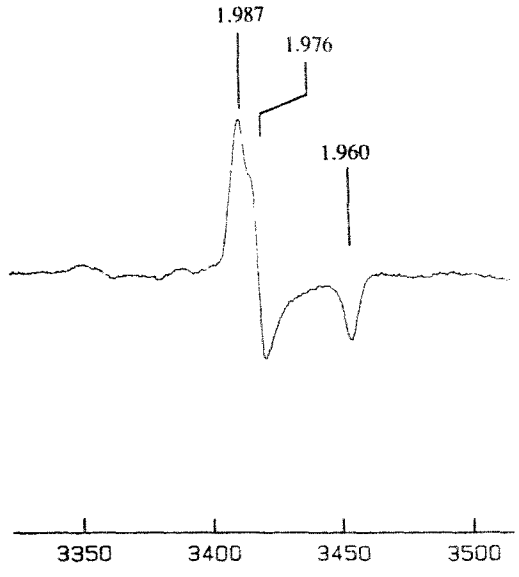

Fig. 8. Mo(V) EPR spectrum of membranes containing over-expressed DMSO reductase poised at an E_h of −84 mV. The spectrum was recorded at 100 K using a microwave power of 20 mW at 9.45 GHz.

Nitrate reductase gives two distinct Mo spectra (high and low pH forms) depending on pH, with an apparent pK_a of 8.2 [93]. This interconversion has been ascribed to a coupled proton in the low pH form which is absent in the high pH form. However, the pK_a was subsequently shown to be affected by the presence of various anions [96] and it was found that both forms demonstrate proton coupling indicating that the change between these two forms is more complex than originally thought. The Mo spectrum of *E. coli* DMSO reductase

TABLE III

EPR parameters and oxidation-reduction potentials of the molydopterin cofactor

	EPR parameters			Potential (mV)		References
	g_1	g_2	g_3	IV/V	V/VI	
E. coli nitrate reductase						
low pH [a]	1.999	1.986	1.963	+180	+220	93, 94
high pH	1.987	1.981	1.961			
E. coli DMSO reductase	1.987	1.976	1.960	−75	−90	27
R. sphaeroides DMSO reductase	1.989	1.977	1.962	+141	+200	95

[a] Interconversion of the low pH ad high pH species has a pK_a of 8.2.

resembles the high pH form of nitrate reductase suggesting that the ligand geometries of these enzymes are similar [27]. DMSO reductases from *E. coli* and *R. sphaeroides* display only one Mo spectrum over a pH range of 5 to 9 [27,95]. Outside this range, the enzymes denature and lose their cofactors. Whereas the *E. coli* DMSO reductase shows no proton coupling, the DMSO reductase from *R. sphaeroides* shows coupling to a single proton, as in nitrate reductase, between pH 5 and 9. The affect of anions on *E. coli* DMSO reductase has not been studied, but the *R. sphaeroides* enzyme shows no change in its EPR spectrum due to anions. These factors suggest that there are significant differences in the environment of the Mo between the DMSO reductases from *E. coli* and *R. sphaeroides*.

Redox titrations of these enzymes have been carried out to determine the mid-point potentials, $E_{m,7}$, of the Mo IV/V and V/VI couples [27,93–95]. These values are listed in Table III. The nitrate reductase $E_{m,7}$ values are high at +180 mV and +220 mV, respectively. This was not unexpected as the $E_{m,7}$ of the nitrate/nitrite couple is +421 mV [94]. The *E. coli* DMSO reductase Mo center has lower mid-point potentials of −75 mV and −90 mV [27], appropriate for the DMSO/DMS $E_{m,7}$ of +160 mV. Thus, although the DMSO and nitrate reductases from *E. coli* may have similar Mo binding geometries, other factors, particularly the electrostatic environment, must influence the $E_{m,7}$ values of the Mo centre. The *R. sphaeroides* enzyme has much higher $E_{m,7}$ values of +141 mV and +200 mV [95]. This enzyme, while catalyzing the same reaction as the *E. coli* enzyme, is very different. It is composed of only one subunit, has no [Fe-S] centers or other prosthetic groups and is located in the periplasm of a photosynthetic bacteria. The mechanism by which it provides energy for cell growth is, therefore, different from the mechanism used by the *E. coli* DMSO reductase, which is bound to the cytoplasmic side of the inner membrane.

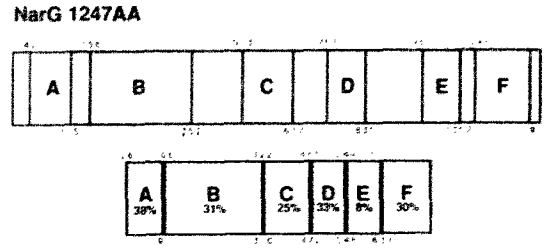

Fig. 9. Regions of similarity between the sequences of the catalytic subunits of nitrate reductase (NarG) and DMSO reductase (DmsA). There are six regions of sequence homology in both sequences, although the intervening sequences are much larger in NarG [19,45,82].

X-C. Sequence analysis of DmsA

DmsA has been shown to have sequence similarity with several Moco-containing prokaryotic enzymes. These include biotin sulfoxide reductase, BisC [97]; nitrate reductases, NarG and NarZ [45,57]; formate dehydrogenase, FdnG [58] of *E. coli*; the formate dehydrogenase of *Methanobacterium formicicum* [98] and the formate dehydrogenase of *Wollinella succinogenes* [99]. These enzymes each have regions of similarity which are easily detected in multiple sequence alignments [19,45,82]. Although NarG and NarZ are consid-

(a)

```
DmsA  26DEKVIWSACTVNCGSRCPLRMHVVDGEIKYV--ETDNTGDDNYDGLHQVPACLRGRSMRRRVYN-----PDRLKYPMKR
NarZ  43HDKIVRSTHGVNCTGSCSWKIYVKNGLVTWEIQQTDYPRTRPDLPNHEPRGCPRGASYSWYLYS-----ANRLKYPLIR
NarG  43HDKIVRSTHGVNCTGSCSWKIYVKNGLVTWETQQTDYPRTRPDLPNHEPRGCPRGASYSWYLYS-----ANRLKYPMMR
FdhF   1--MKKVVTVCPYCASGCKINLVVDNGKIVRA--------EAAQGKTNQGTLCLKG-YYGWDFINDTQILTPRLKTPMIR
FdhAM  1-DIKYVPTICPYCGVGCGMNLVVKDEKVVGV-------EPWKRHPVNEGKLCPKG-NFCYEIIH----REDRLTTPLIK
FdhAW 52--SKKVKTICTYCSVGCGIIAEVVDGVWVRQ-------EVAQDHPISQGGHCCKGADMIDKARS-----ETRLRYPIEK
FdnG  42-RAKEIRNTCTYCSVGCGLLMYSLGDGAKNAREAIYHIEGDPDHPVSRGALCPKGAGLLDYVNSE-----NRLRYPEYR
BisC   1-------------------------------------------------MENSLQSAVRDQVHS-----NTRVRFPMVR
```

(b)

```
CONSENSUS

(S)-(C)(2:3)C---C(var)C-(R)G(var)R(Hydro)(R)-P--(R)
 T   H            26:34   K  11:15          K      K
```

Fig. 10. (a) Sequence alignment of the putative molybdopterin-binding domain in NarZ [102], NarG [45], FdhF [58], FdhA from *Methanobacterium formicicum* [96], FdhA from *Wollinella succinogenes* [99], FdnG [58] and BisC [97]. (b) Consensus sequence for the putative molybdopterin binding domain.

erably larger than DmsA, there are six blocks of similar sequence distributed throughout the polypeptides (Fig. 9).

The site of Moco binding is presumably in one or a combination of these regions of homology. Examination of the sequences has allowed us to identify a group of invariant residues in the amino proximal region (Fig. 10) which is present in seven of the eight available sequences and partially observed in the eighth sequence. The N-terminal part of this motif (Moco motif), containing three invariant Cys residues, is absent in BisC (Fig. 10). It should be noted that all the polypeptides except BisC are part of multi-subunit complexes and communicate with [Fe-S] clusters in an electron-transfer subunit. BisC receives electrons from a poorly understood thioredoxin-like protein [97]. We suggest that the cluster of three Cys residues is required for subunit-subunit interaction and/or electron-transfer, whereas the C-terminal part of the Moco motif, present in all eight sequences, is required for Moco attachment. This part contains a number of basic residues which could ligate the negative phosphate groups of the cofactor.

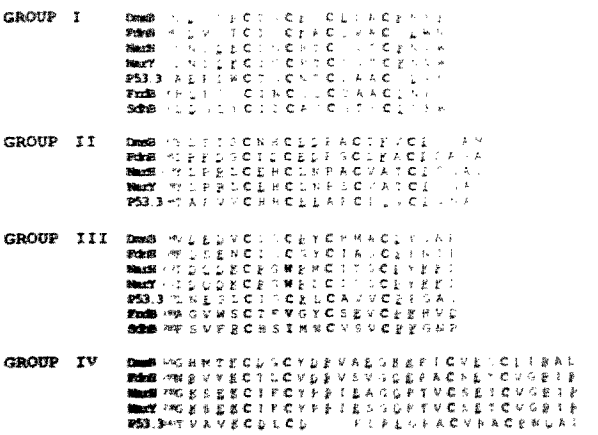

Fig. 11. Sequence alignment for the putative [Fe-S] cluster binding sequences of DmsB with related [Fe-S] proteins [58,45,102–105]. The sequences from FrdB, SdhB, NarH, and NarY corresponding to the sequence of Cys group III from DmsB ligate [3Fe-4S] clusters. The remaining sequences ligate [4Fe-4S] clusters. Charged residues and Pro residues following the fourth Cys of each group are underlined.

XI. DmsB

XI-A. DmsB is an [Fe-S] protein

DMSO reductase, fumarate reductase, nitrate reductase, formate dehydrogenase, and succinate dehydrogenase share a common structural design incorporating catalytic, electron-transfer and membrane anchor subunits [2,39,56]. In each case, the electron-transfer subunit has multiple Cys residues in sequence groups very similar to those that have been shown to ligate [Fe-S] clusters in the bacterial ferredoxins [100,101] (Fig. 11). The presence of [Fe-S] clusters in the electron-transfer subunits of fumarate reductase and succinate dehydrogenase have been verified using a combination of biophysical techniques and molecular genetics [106–108]. The sequence of DmsB contains four Cys groups which are similar to those found in proteins known to contain [4Fe-4S] clusters [19]. Fig. 11 shows a comparison of the four Cys groups of DmsB with the equivalent groups of NarH [45], NarY [98], FrdB [103], SdhB (the electron-transfer subunit of succinate dehydrogenase) [99], FdnH and a polypeptide of unknown function, encoded by a gene at 53.3′ on the *E. coli* chromosome [105].

The EPR properties of the purified and in situ DMSO reductase have recently been reported [27]. DmsB appears to contain four [4Fe-4S] clusters, and this results in the observation of a complex EPR spectrum (Fig. 12) [27,109] in the fully reduced state which has features similar to spectra of other proteins containing multiple [4Fe-4S] clusters, such as *Clostridium pasteurianum* ferredoxin [110] and *Micrococcus lacti-lyticus* ferredoxin [111]. Because of the magnetic interactions between the reduced clusters, it is not possible to assign the features of the fully reduced spectrum to individual clusters of the enzyme. However, the spectrum can be loosely interpreted in terms of two pairs of interacting [4Fe-4S] clusters, with each pair having spectroscopic similarities with the bacterial eight-iron ferredoxins. The EPR spectrum of fully reduced DMSO reductase is quite distinct from the spectra reported for nitrate reductase from *E. coli* [93,94,112] and *Bacillus halodenitrificans* [113].

XI-B. Redox properties of the [Fe-S] clusters

Cammack and Weiner [27] analysed the EPR spectra of DMSO reductase potentiometrically, and found that the [Fe-S] clusters of the enzyme titrated with four mid-point potentials at pH 7 ($E_{m,7}$) of −50, −120, −240 and −330 mV. Spin quantitations indicated that the enzyme contains a total of four [4Fe-4S] clusters in addition to the single molybdopterin cofactor described above (subsection XB).

DMSO reductase catalyzes the two-electron reduction of a range of S- and N-oxide compounds, but the total number of electrons able to be carried at any time excluding MQH_2 and $MQ^{\cdot-}$ species is six: one in each of the [4Fe-4S] clusters and two in the molybdopterin. Since only two electrons are utilized per reaction cycle (i.e., the two electron reduction of DMSO), this suggests that not all of the [4Fe-4S] clusters may be active in the redox cycle of the enzyme. The enzyme catalyzes electron-transfer from MQH_2 with a $E_{m,7}$ of −74 mV (MQH_2/MQ, average for the two one-electron transfers) [42] to DMSO with an $E_{m,7}$ of +160 mV (DMSO/DMS). This suggests that the −330 mV and

−240 mV clusters may not be directly involved in enzyme turnover. A similar situation exists for *E. coli* fumarate reductase. FrdB contains three [Fe-S] clusters: FR1 ([2Fe-2S]; $E_{m,7}$, −20 mV), FR2 ([4Fe-4S]; $E_{m,7}$, −330 mV) and FR3 ([3Fe-4S]; $E_{m,7}$ = −70 mV; [2]). In this case electrons are transferred from MQH_2 ($E_{m,7}$, −74 mV) to fumarate (fumarate/succinate; $E_{m,7}$, +30 mV), and one of the clusters (FR2) appears to have a midpoint potential too low to be directly involved in the redox cycle of the enzyme.

The role of the low potential clusters in both DMSO reductase and fumarate reductase remains elusive. If DmsB and FrdB evolved from ferredoxin-like proteins [114], the presence of the low potential clusters may simply be an artifact. Alternatively, because [Fe-S] clusters are able to bring together regions of sequence into a defined conformation, it is possible that these clusters serve a structural role.

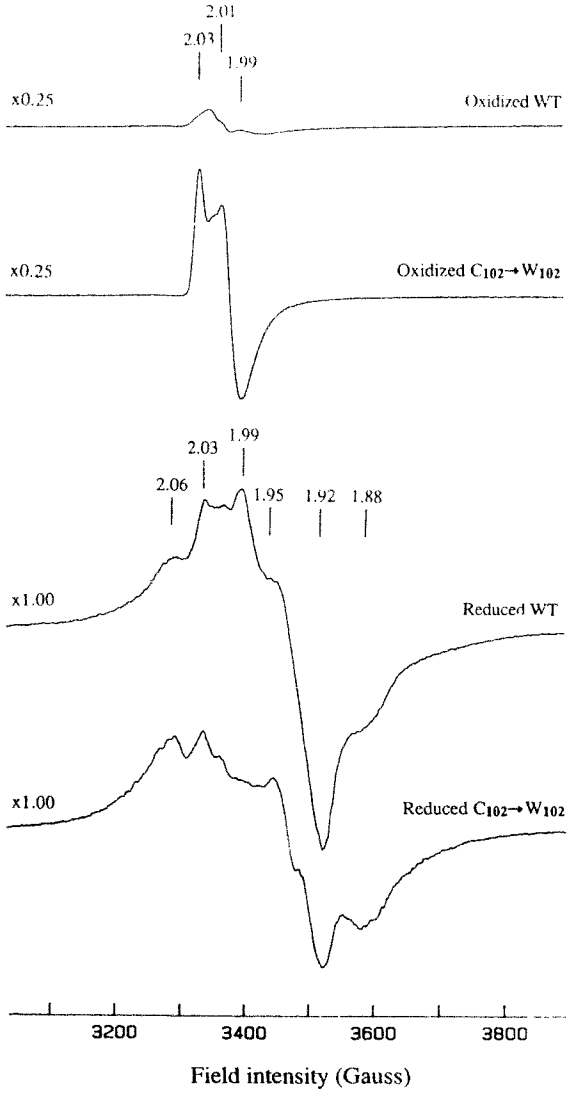

Fig. 12. [Fe-S] EPR spectrum of membranes containing over-expressed wild-type and mutant DMSO reductase (subsection XId). Oxidised samples were oxidised with ferricyanide, reduced samples were reduced with dithionite. Spectra were recorded at 12 K using a microwave power of 20 mW at 9.45 GHz.

XI-C. Comparison with other [Fe-S] proteins

E. coli is capable of synthesizing two distinct respiratory nitrate reductases; these are the major NarGHJI and minor NarZYWV enzymes [45,102]. Both enzymes are very similar in terms of catalytic/electron-transfer subunit composition to *E. coli* DMSO reductase. In addition to the similarities shown with NarH, NarY, FrdB and SdhB the following similarities exist with the bacterial ferredoxins [45]:

Groups I and III: Similarity with the consensus [4Fe-4S] ferredoxin Cys group motif CxxCxxCxxxCP [100,101], although group I has a Lys in place of the Pro.

Group II: Similarity with *Azotobacter vinelandii* ferredoxin I ([4Fe-4S]) and *Ps. ovalis* ferredoxin ([4Fe-4S], [100]).

Group IV: Similarity with *Chromatium vinosum* ferredoxin ([4Fe-4S]; [100]). In this case the similarity is not as strong as those found for groups I-III, as the spacing between the second and third Cys residues is 8 in *C. vinosum* ferredoxin and 11 in DmsB group IV.

In the case of the bacterial eight-iron ferredoxins (which contain two [4Fe-4S] clusters) for which X-ray structures are known, it is found that the first three Cys residues of each group ligate one [4Fe-4S] cluster, while the fourth Cys provides the fourth ligand to the other [4Fe-4S] cluster in the protein [98,99]. Consideration of the spacing of the Cys groups of DmsB and the spacing found in the bacterial ferredoxins allows a model to be proposed for the interaction of the Cys residues of DmsB with the four [4Fe-4S] clusters observed by Cammack and Weiner [27] (Fig. 13).

NarH (502 residues) and NarY (514 residues) are both much larger subunits than DmsB (207 residues). Despite this, the ferredoxin-like sequence groups are almost identical to those found in DmsB (Fig. 11). There are larger gaps between the first and second Cys groups in NarH and NarY than in DmsB, and there are much longer C-terminal sequences beyond Cys group IV in the two nitrate reductases. The only major difference in Cys group composition is in Cys group III, where the residue equivalent to Cys_{102} of DmsB is replaced by a Trp residue in NarH and NarY. This results in NarH (and probably NarY) having a [3Fe-4S] cluster ligated primarily by this Cys group, rather than the [4Fe-4S] cluster found in DmsB.

E. coli nitrate reductase, NarGHJI, has been characterized using EPR and magnetic circular dichroism

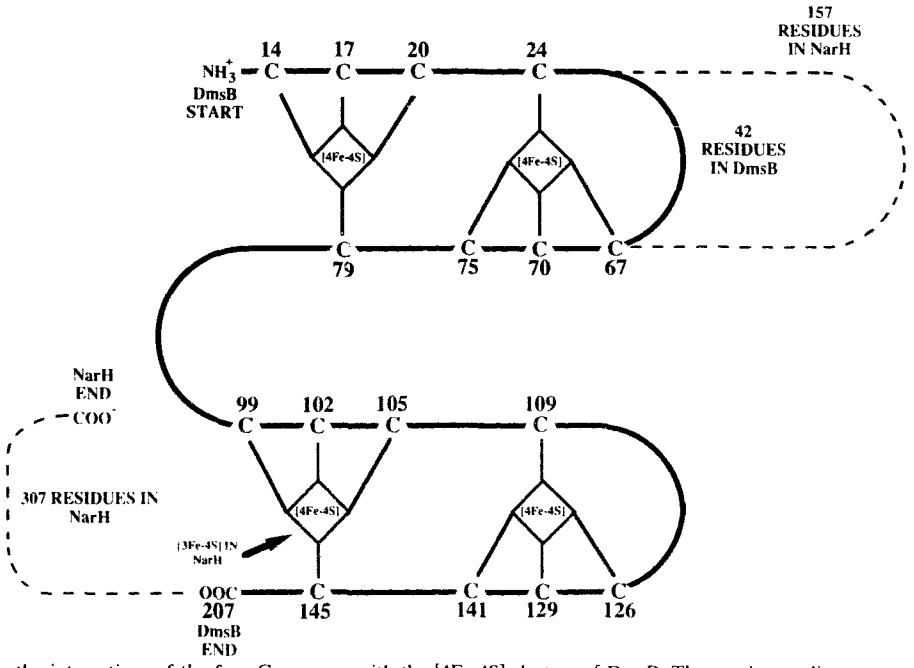

Fig. 13. Model for the interactions of the four Cys groups with the [4Fe-4S] clusters of DmsB. The continuous line represents DmsB, and the dashed line represents the major differences between the sequence of DmsB and NarH. The model is based on comparisons with the sequences of the bacterial ferredoxins [100,101].

(MCD) spectroscopies [93,94,112]. Johnson et al. [112] showed by EPR and MCD that purified nitrate reductase contains between three and four [4Fe-4S] clusters and one [3Fe-4S] cluster. Vincent [94] studied the potentiometric behaviour of the purified enzyme, and determined $E_{m,7}$ values of the molybdopterin Mo(IV/V) and Mo(V/VI) couples and the [Fe-S] clusters. The signals corresponding to the [4Fe-4S] clusters titrated with a single $E_{m,7}$ value of +80 mV, whereas the signal corresponding to the [3Fe-4S] cluster titrated with an $E_{m,7}$ value of +50 mV. The observation of only a single $E_{m,7}$ value associated with the [4Fe-4S] clusters is apparently inconsistent with the data of Johnson et al. [112]. The presence of multiple clusters with identical $E_{m,7}$ values, differences in enzyme preparations, or lack of available potentiometric data at potentials lower than −100 mV, may explain the data reported by Vincent [94]. The enzyme from *Bacillus halodenitrificans* has also been characterized by EPR [113] and has been reported to contain both [4Fe-4S] and [3Fe-4S] clusters, similar to the NarGHJI enzyme from *E. coli*.

XI-D. Oligonucleotide-directed mutagenesis of the Cys groups

Construction of oligonucleotide-directed mutants of the conserved Cys residues in *E. coli* fumarate reductase [107] and *A. vinelandii* ferredoxin I [115] have recently been reported. Werth et al. [107] mutated the four N-terminal Cys residues in FrdB, which have a sequence similar to the the Cys groups ligating the [2Fe-2S] clusters of the plant ferredoxins. In this case, each of the four Cys residues were mutagenized to Ser residues. The resultant mutants retained cluster FR1, but the cluster had altered redox and EPR properties, depending on which Cys residue was mutagenized. The properties of the FR2 [4Fe-4S] and the FR3 [3Fe-4S] clusters were unchanged.

Martin et al. [115] have reported oligonucleotide-directed mutagenesis of one of the Cys residues providing ligands to the [4Fe-4S] cluster of *A. vinelandii* ferredoxin I. Cys_{20} was changed to an Ala residue, and the mutant protein retains the [4Fe-4S] cluster by using a redundant Cys elsewhere in the sequence (Cys_{24}) to replace Cys_{20}. This causes minor changes in the structure of the protein, as well as minor changes in the EPR spectrum of the [3Fe-4S] cluster (the [4Fe-4S] cluster is not reducible by dithionite).

We have recently constructed a series of mutants in the Cys residues of DmsB [109]. We have found that changing Cys_{102} to a Trp, Ser, Phe, or Tyr results in the replacement of the [4Fe-4S] cluster ligated primarily by Cys group III with a [3Fe-4S] cluster which is EPR detectable in its oxidized state (Fig. 12) [109]. This is the first report in the literature of a [4Fe-4S] to [3Fe-4S] conversion being induced by oligonucleotide-directed mutagenesis.

The Cys_{102} mutant enzymes also have altered EPR spectra in their reduced states [109]. The mutant enzymes all assemble into the cytoplasmic membrane, but

they do not support growth on glycerol-DMSO minimal media. These results indicate the importance of the [4Fe-4S] cluster to which Cys_{102} of DmsB provides a ligand to the overall function of DMSO reductase in electron-transfer from MQH_2 to DMSO. However, all of the mutants have high BV_{red}: DMSO oxidoreductase activities, indicating that the pathway of electrons from BV_{red} to DMSO is distinct from that of electrons from MQH_2 to DMSO.

XII. DmsC

DmsC is a polypeptide of M_r 30789 with a high proportion of hydrophobic and nonpolar amino acids. Hydropathy analysis of the protein indicates that DmsC has eight stretches of hydrophobic residues each of 20 ± 4 residues [19]. These stretches are capable of forming transmembranal α-helical segments. Analysis by the Kyte-Doolittle and Rao-Argos algorithms and by the membrane preference scale devised by degli Esposti [116] supports the presence of eight hydrophobic segments.

XII-A. Anchor junction

Several lines of evidence support an anchor function for DmsC. Disruption of *dmsC* in the cloned *dms* operon by transposon Tn5 insertion mutagenesis results in the accumulation of soluble DMSO reductase in the cytoplasm. This has been confirmed by constructing chromosomal deletion mutants of DmsC, which accumulate soluble DMSO reductase. Also, based on immunogold electronmicroscopy, it seems likely that the DmsAB catalytic dimer is held to the membrane by DmsC [26].

We have constructed a number of alkaline phosphatase, *phoA*, fusions to *dmsC*. Fusions which disrupt the *dmsC* gene produce an inactive anchor and soluble catalytically active DmsAB. We have obtained one fusion in which *phoA* is inserted in the termination codon. This creates a chimeric subunit with full length *dmsC* and *phoA*. The chimeric enzyme has membrane-bound DMSO reductase activity, which is able to support growth on DMSO. More fusions must be analyzed before this technique can provide a model for the transmembranal topology of DmsC (G.S. and J.H.W., unpublished results).

XII-B. DmsC is required for quinol oxidation and thermostability

In addition to the obvious anchor role of DmsC, we have found two additional activities for this subunit. DmsC is required for MQH_2 oxidase activity and stability of the enzyme. Only trimeric holoenzyme is able to oxidize a soluble analogue of MQH_2, $DMNH_2$. Although the DmsAB dimer catalyzes BV_{red} oxidation, it is inactive with $DMNH_2$ [39]. This property resembles the activity of fumarate reductase in which FrdAB has BV_{red} oxidase activity but lacks $DMNH_2$ oxidase activity [56,117,118]. In fumarate reductase we have identified His_{82} of FrdC as a key residue in MQH_2 oxidation. This His appears to reside very close to the membrane-cytoplasm interface in the sequence: ^{78}*Ala-Ala*-Leu-*Leu-His*-Thr-Lys-*Thr* and a mutation was found in which His_{82} was changed to Arg. This mutant was unable to grow on fumarate, retained normal BV_{red} oxidase activity but totally lacked $DMNH_2$ oxidase activity [117]. DMSO reductase has a very similar sequence: ^{61}*Ala-Ser*-Met-*Leu-His*-Leu-Gly-*Ser* in which His_{65} would occupy a position close to the membrane/aqueous interface. We have changed His_{65} to Arg and have found that this mutant is unable to grow on DMSO but retains BV_{red} oxidase activity. This suggests that this region of DmsC is involved in MQH_2 binding and oxidase activity (R.A.R. and J.H.W., unpublished results.)

DmsC has also been found to stabilize the DmsAB catalytic dimer to thermal inactivation at 30°C [39]. The anchor subunits of fumarate reductase, FrdCD, stabilize the thermolability and alkali sensitivity of the catalytic FrdAB dimer.

XIII. Summary and perspectives

Studies on the DMSO reductase of *E. coli* have produced new insights into membrane protein structure, mechanisms of electron transfer, the redox properties of [Fe-S] clusters and molybdenum cofactors and bacterial bioenergetics. This complex enzyme can be readily expressed to high levels providing sufficient material for biochemical and biophysical studies and the genes encoding the subunits can be modified by site-directed mutagenesis. We expect that the combination of these features will lead in the near future to detailed understanding of the ligation of Moco to the polypeptide. The presence of multiple [Fe-S] clusters offers opportunities to study the organization, environment and factors which modulate the redox potential of these important electron transfer cofactors. We also expect that site-directed mutagenesis will help unravel the mechanism of MQH_2 binding and the flow of electrons and protons within the enzyme and across the membrane. We hold out the possibility of obtaining three-dimensional structural information on this enzyme by X-ray crystallography or electron diffraction of two-dimensional arrays.

Acknowledgments

Work in the author's laboratory was supported by the Medical Research Council of Canada and by the Al-

berta Heritage Foundation for Medical Research. CAT and RAR were supported by AHFMR. The authors would like to thank Prof. D.G. Scraba for electron microscopic studies and Dr. R.J. Turner for computer analyses of the sequence of DmsC.

References

1 Lin, E.C.C. ad Kuritzkes, D.R. (1987) in *Escherichia coli* and *Salmonella typhimurium* (Neidhardt, F.C., ed.), Vol. I, pp. 201–221, Am. Soc. Microbiol., Washington, DC.
2 Cole, S.T., Condon, C., Lemire, B.D. and Weiner, J.H. (1985) Biochim. Biophys. Acta 811, 381–403.
3 Stewart, V. (1988) Microbiol. Rev. 52, 190–232.
4 Barrett, H.S. and Kwan, H.S. (1985) Annu. Rev. Microbiol. 39, 131–149.
5 Zinder, S.H. and Brock, T.D. (1978) J. Gen. Microbiol. 105, 335–342.
6 Bilous, P.T. and Weiner, J.H. (1985) J. Bacteriol. 162, 1151–1155.
7 Bilous, P.T. and Weiner, J.H. (1988) J. Bacteriol. 170, 1511–1518.
8 Weiner, J.H., MacIsaac, D.P., Bishop, R.E. and Bilous, P.T. (1988). J. Bacteriol. 170, 1505–1510.
9 Zeyer, J., Eicher, P., Wakeham, S.G. and Schworzenbach, R.P. (1987) Appl. Env. Microbiol. 53, 2026–2032.
10 Kiene, R.P. and Bates, T.S. (1990) Nature 345, 702–704.
11 Lovelock, J.E., Maggs, R.J. and Ramussen, R.A. (1972) Nature 237, 452–453.
12 Kellogg, N.W., Cadle, R.D., Allen, E.R., Lazrus, A.L. and Martell, E.A. (1972) Science 175, 587–596.
13 Andreae, M.O. (1980) Limnol. Oceanogr. 25, 1054–1063.
14 Oren, A. and Truper, H.G. (1990) FEMS Microbiol. Lett. 70, 33–36.
15 Styrvold, O.B. and Strøm, A.R. (1984) Arch. Microbiol. 140, 74–78.
16 Satoh, T. and Kurihara, F.N. (1987) J. Biochem. 102, 191–197.
17 McEwan, A.G., Wetzstein, H.G., Meyer, O., Jackson, J.B. and Ferguson, S.J. (1987) Arch. Microbiol. 147, 340–345.
18 Selander, R.K., Gaugant, D.A., and Whittam, T.S. (1987) in *Escherichia coli* and *Salmonella typhimurium* (Neidhardt, F.C., ed.), Vol. II, pp. 1625–1648, Am. Soc. Microbiol., Washington, DC.
19 Bilous, P.T., Cole, S.T., Anderson, W.F. and Weiner, J.H. (1988) Mol. Microbiol. 2, 785–795.
20 Schultz, J.E. and Weaver, P.F. (1982) J. Bacteriol. 149, 181–190.
21 Sagai, M. and Ishimoto, M. (1973) J. Biochem. 73, 843–859.
22 Silvestro, A., Pommier, J. and Giordano, G. (1988) Biochim. Biophys. Acta 954, 1–13.
23 Kwan, H.S. and Barrett, E.L. (1983) J. Bacteriol. 155, 1455–1458.
24 McEwan, A.G., Ferguson, S.J., and Jackson, J.B. (1991) Biochem. J. 274, 305–307.
25 Bilous, P.T. and Weiner, J.H. (1985) J. Bacteriol. 163, 369–375.
26 Sambasivarao, D., Scraba, D.G., Trieber, C. and Weiner, J.H. (1990) J. Bacteriol. 172, 5938–5948.
27 Cammack, R. and Weiner, J.H. (1990) Biochemistry 29, 8410–8416.
28 Shimakawa, O. and Ishimoto, M. (1979) J. Biochem. 86, 1709–1717.
29 Takagi, M., Tsuchiya, T. and Ishimoto, M. (1981) J. Bacteriol. 148, 762–768.
30 Bragg, P.D. and Hackett, N.R. (1983) Biochim. Biophys. Acta 725, 168–177.
31 Sambasivarao, D. and Weiner, J.H. (1991) Curr. Microbiol. 23, 105–110.
32 Stenberg, E., Styrvold, O.B. and Strøm, A.R. (1982) J. Bacteriol. 149, 22–28.
33 Easter, M.C., Gibson, D.M. and Ward, F.B. (1983) J. Gen. Microbiol. 129, 3689–3696.
34 McEwan, A.G., Wetzstein, H.G., Ferguson, S.J. and Jackson, J.B. (1985). Biochim. Biophys. Acta 806, 410–417.
35 Kurihara, F.N. and Satoh, T. (1988) Plant. Cell. Physiol. 29, 377–379.
36 Unemoto, T., Hayashi, M., Miyaki, K. and Hayashi, M. (1965). Biochim. Biophys. Acta. 110, 319–328.
37 Silvestro, A., Pommier, J., Pascal, H.C. and Giordano, G. (1989). Biochim. Biophys. Acta 999, 208–216.
38 Yamamoto, I., Hinakura, M., Seki, S., Seki, Y. and Kondo, H. (1990). Curr. Microbiol. 20, 245–249.
39 Sambasivarao, D. and Weiner, J.H. (1991) J. Bacteriol. 173, 5935–5943.
40 Daruwala, R. and Meganathan, R. (1991) FEMS Microbiol. Lett. 83, 255–260.
41 Yamamoto, I., Hinakura, M., Seki, S., Seki, Y. and Kondo, H. (1989) J. Gen. Appl. Microbiol. 35, 253–259.
42 Ingledew, W.J. and Poole, R.K. (1984) Microbiol. Rev. 48, 222–271.
43 Cox, J.C. and Knight, R. (1981) FEMS Microbiol. Lett. 12, 249–252.
44 Meganathan, R. (1984) FEMS Microbiol. Lett. 24, 57–62.
45 Blasco, F., Iobbi, C., Giordano, G., Chippaux, M. and Bonnefoy, V. (1989) Mol. Gen. Genet. 218, 249–256.
46 McEwan, A.G., Richardson, D.J., Hudig, H., Fergusson, S.J. and Jackson, J.B. (1989) Biochim. Biophys. Acta 973, 308–214.
47 Brice, J.M., Law, J.F., Meyer, D.J. and Jones, C.W. (1974). Biochem. Soc. Trans. 2, 523–526.
48 Gutowski, S.J. and Rosenberg, H. (1977) Biochem. J. 164, 265–267.
49 Myers, C.R. and Nealson, K.H. (1990) J. Bacteriol. 172, 6232–6238.
50 Eiglmeier, K., Honoré, N., Iuchi, S., Lin, E.C.C. and Cole, S.T. (1989). Mol. Microbiol. 3, 869–878.
51 Spiro, S. and Guest, J.R. (1991) Trends Biochem. Sci. 16, 310–314.
52 Spiro, S. and Guest, J.R. (1990) FEMS Microbiol. Rev. 75, 399–428.
53 Iuchi, S. and Lin, E.C.C. (1987) Proc. Natl. Acad. Sci. USA 84, 3901–3905.
54 Iuchi, S. and Lin, E.C.C. (1991) Cell 66, 5–7.
55 Egan, S.M. and Stewart, V. (1990) J. Bacteriol. 172, 5020–5029.
56 Condon, C. and Weiner, J.H. (1988) Mol. Microbiol. 2, 43–52.
57 Bonnefoy, V., Burini, J.F., Giordano, G., Pascal, M.C. and Chippaux, M. (1987) Mol. Microbiol. 1, 143–150.
58 Berg, B.L., Li, J., Heider, J., and Stewart, V. (1991) J. Biol. Chem., in the press.
59 Blasco, F., Pommier, J., Augier, M., Chippaux, M. and Giordano, G. (1992) Mol. Microbiol. 6, 221–230.
60 Dubourdieu, M. and DeMoss, J.A. (1992) J. Bacteriol. 174, 867–872.
61 Melville, S.B. and Gunsalus, R.P. (1990) J. Biochem. 265, 18733–18736.
62 Pascal, M.C., Burini, J.F. and Chippaux, M. (1984) Mol. Gen. Genet. 195, 351–355.
63 Gennis, R.B. (1987) FEMS Microbiol. Rev. 46, 381–389.
64 Frey, B., Janel, G., Michelson, U. and Kerstein, H. (1989) J. Bacteriol. 171, 1524–1530.
65 Trageser, M., Spiro, S., Duchene, A., Kojro, E., Fahrenholz, F., Guest, J.R. and Unden, G. (1990) Mol. Microbiol. 4, 21–27.
66 Shaw, D.J., Rice, D.W. and Guest, J.R. (1983) J. Mol. Biol. 166, 241–247.
67 Unden, G. and Duchene, A. (1987) Arch. Microbiol. 147, 195–200.
68 Unden, G., Trageser, M. and Duchene, A. (1990) Mol. Microbiol. 4, 315–319.

69 Green, J., Trageser, M., Six, S., Unden, G. and Guest, J.R. (1991). Proc. Roy. Soc. Lond. 244, 137–144.
70 Spiro, S. and Guest, J.R. (1988) Mol. Microbiol. 2, 701–707.
71 Kiley, P.J. and Reznikoff, W.A. (1991) J. Bacteriol. 173, 16–22.
72 Spiro, S. and Guest, J.R. (1987) Mol. Microbiol. 1, 53–58.
73 Cotter, P.A. and Gunsalus, R.P. (1989) J. Bacteriol. 171, 3817–3823.
74 Kalman, L.V. and Gunsalus, R.P. (1990) J. Bacteriol. 172, 7049–7056.
75 Forst, S., Delgado, J. and Inouye, M. (1989) Proc. Natl. Acad. Sci. USA 86, 6052–6056.
76 Hess, J.F., Oosawai, K., Matsumuta, P. and Simon, M.I. (1987). Proc. Natl. Acad. Sci. USA 84, 7609–7613.
77 Iuchi, S. and Lin, E.C.C. (1987) J. Bacteriol. 169, 3720–3725.
78 Shine, J. and Dalgarno, L. (1974) Proc. Natl. Acad. Sci. USA 71, 1342–1346.
79 Yamamoto, I., Yamazaki, N., Hohmura, M. and Ishimoto, M. (1990) J. Gen. Appl. Microbiol. 36, 357–363.
80 Pascal, M.C., Lepelletier, M., Giordano, G. and Chippaux, M. (1991) FEMS Microbiol. Lett. 78, 297–300.
81 Sambasivarao, D., Scraba, D.G. and Weiner, J.H. (1988) EBEC Short Rep. 5, 149.
82 Wootton, J.C., Nicolson, R.E., Cock, J.M., Waters, D.E., Burke, J.F., Doyle, W.A. and Bray, R.C. (1991) Biochim. Biophys. Acta 1057, 157–185.
83 Johnson, M. and Rajagopalan, K. (1987) J. Bacteriol. 169, 117–125.
84 Johnson, J.L., and Rajagopalan, K.V. (1982) Proc. Natl. Acad. Sci. USA 79, 6856.
85 Johnson, J.L., Hainline, K.V., Rajagopalan, K.V., and Arison, B.H. (1984) J. Biol. Chem. 259, 5414–5422.
86 Kramer, S., Johnson, J., Ribeiro, A., Millington, D. and Rajagopalan, K. (1987) J. Biol. Chem. 262, 16357–16363.
87 Johnson, J.L., Bastian, N.R. and Rajagopalan, K.V. (1990) Proc. Natl. Acad. Sci. USA 87, 3190–3194.
88 Karrassch, M., Borner, G. and Thauer, R. (1990) FEBS Lett. 274, 48–52.
89 Johnson, J., Bastian, N., Schauer, N., Ferry, J. and Rajagopalan, K (1991) FEMS Microbiol. Lett. 77, 213–216.
90 Johnson, J., Indermaur, L. and Rajagopalan, K. (1991) J. Biol. Chem. 266, 12140–12145.
91 Börner, G., Karrasch, M., and Thauer, R.K. (1991) FEBS Lett. 290, 31–34.
92 Amy, N. and Rajagopalan, V. (1979) J. Bacteriol. 140, 114–124.
93 Vincent, S. and Bray, R. (1978) Biochem. J. 171, 639–647.
94 Vincent, S. (1979) Biochem. J. 177, 757–759.
95 Bastian, N., Kay, C., Barber, M. and Rajagopalan, K. (1991) J. Biol. Chem. 266, 45–51.
96 George, G., Bray, R., Morpeth, F. and Boxer, D. (1985) Biochem. J. 227, 925–931.
97 Pierson, D.E. and Campbell, A. (1990) J. Bacteriol. 172, 2194–2198.
98 Schuber, A.P., Orr, R.C., Recny, M.A., and Schendel, P.F. (1986). J. Biol. Chem. 261, 12942–12947.
99 Bokranz, M., Guttman, M., Kortner, C., Kojro, F., Fahrenholz, F., Lauterbach, F., and Kröger, A. (1991) Arch. Microbiol. 156, 119–128.
100 Bruschi, M. and Guerlesquin, F. (1988) FEMS Microbiol. Rev. 54, 155–176.
101 George, D.G., Hunt, L.T., Yeh, L.L. and Barker, W.C. (1985) J. Mol. Evol. 22, 20–31.
102 Blasco, F., Iobbi, C., Ratouchniak, J., Bonnefoy, V. and Chippaux, M. (1990) Mol. Gen. Genet. 222, 104–111.
103 Cole, S.T., Grundstrom, T., Jaurin, B., Robinson, J.J. and Weiner, J.H. (1982) Eur. J. Biochem. 126, 211–216.
104 Darlison, M.G. and Guest, J.R. (1984) Biochem. J. 233, 507–517.
105 Andrews, S.C., Harrison, P.M. and Guest, J.R. (1991) J. Gen. Microbiol. 137, 361–367.
106 Johnson, M.K., Kowal, A.T., Morningstar, J.E., Oliver, M.E., Whittaker, K., Gunsalus, R.P., Ackrell, B.A.C. and Cecchini, G. (1988) J. Biol. Chem. 263, 14732–14738.
107 Werth, M.T., Cecchini, G., Manadori, A., Ackrell, B.A.C., Schroder, I., Gunsalus, R.P. and Johnson, M.K. (1990) Proc. Natl. Acad. Sci. USA 87, 8965–8969.
108 Maguire, J.J. and Hederstedt, L. (1989) FEBS Lett. 256, 195–199.
109 Rothery, R.A. and Weiner, J.H. (1991) Biochemistry 30, 8296–8305.
110 Prince, R.C. and Adams, M.W.W. (1987) J. Biol. Chem. 262, 5125–5128.
111 Mathews, R., Charlton, S., Sands, R.H. and Palmer, G. (1974) J. Biol. Chem. 249, 4326–4328.
112 Johnson, M.K., Bennett, D.E., Morningstar, J.E., Adams, M.W.W. and Mortenson, L.E. (1985) J. Biol. Chem. 260, 5456–5463.
113 Ketchum, P.A., Denariaz, G., LeGall, J., and Payne, W.J. (1989). J. Bacteriol. 173, 2498–2505.
114 Cammack, R. (1986) in Iron-sulfur protein research (Matsubara, H., Katsube, Y., and Wada, K, eds.), pp 40–55, Springer, Berlin.
115 Martin, A.E., Burgess, B.K., Stout, C.D., Cash, V.L., Dean, D.R., Jensen, G.M. and Stephens, P.J. (1990) Proc. Natl. Acad. Sci. USA 87, 598–602.
116 Degli Esposti, M. (1989) Biochim. Biophys. Acta 977, 249–265.
117 Weiner, J.H., Cammack, R., Cole, S.T., Condon, C., Honoré, N., Lemire, B.B. and Shaw, G. (1986) Proc. Natl. Acad. Sci. USA 83, 2056–2060.
118 Westenberg, D.J., Gunsalus, R.P., Ackrell, B.A.C. and Cecchini, G. (1990) J. Biol. Chem. 265, 19560–19567.